The origins of friction and the growth of graphene, investigated at the atomic scale

Baarle, D.W. van

Cover Page

Universiteit Leiden

The handle http://hdl.handle.net/1887/44539 holds various files of this Leiden University dissertation.

Author: Baarle, D.W. van
Title: The origins of friction and the growth of graphene, investigated at the atomic scale
Issue Date: 2016-11-29

Part I

On the origins of friction

Chapter 1

Introduction and motivation

1.1 Hunting for the fundamentals of friction

1.1.1 A historical note

Friction is an everyday life phenomenon. The first research on friction was performed in the 15th century by Leonardo Da Vinci, resulting in the first friction laws. Da Vinci's unpublished findings have been repeated independently in the 18th century by Amontons and Coulomb[2]. The resulting Amontons-Coulomb law states that the kinetic friction force between two sliding macroscopic objects is given by

$$F = \mu N \tag{1.1}$$

with N being the normal load, i.e. the force with which the two bodies are pressed against each other, and μ the macroscopic friction coefficient. One of the most remarkable aspects of this relation is the absence of both the real or apparent contact area (see Figure 1.1) and the relative velocity between the two sliding objects. The absence of the apparent contact area in Equation 1.1 can be explained by focussing on the real contact between the two bodies. As illustrated in Figure 1.1, the real contact is formed by the ensemble of asperities on the two surfaces that mechanically touch the opposite surface[3]. Plastic and elastic deformations of the asperities under the applied normal load lead to a total contact area that is more or less proportional to that load. If we assume that the friction force, i.e. the lateral force required to make the interface slip, is proportional to the real area of contact, the proportionality between the normal force and the real contact area makes the friction force directly proportional to the loading force, in accordance with Equation 1.1.
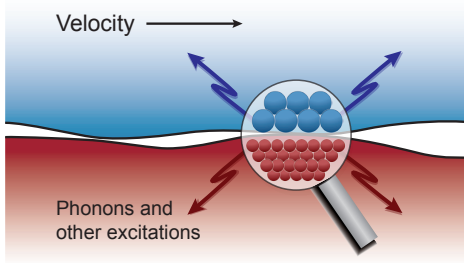
Figure 1.1: Schematic view of the interface between two macroscopic bodies. On the microscale, only a small fraction of the apparent contact area is in genuine, mechanical contact. This real contact area is established by a large number of microscopic asperities.

1.1.2 Experimental studies of a single asperity

When one realizes that a friction contact is formed by an ensemble of small asperities, it is straightforward to study the properties of one single asperity in order to research the origins of friction. The invention of the Atomic Force Microscope (AFM) has resulted in a tool that allows one to study friction at the atomic scale using its tip as a single-asperity contact[4]. This has resulted in the development of a special type of AFM, tailored to investigate atomic-scale friction, known as the Friction Force Microscope (FFM) or Lateral Force Microscope (LFM). A two-dimensionally sensitive LFM has been constructed by our research group[5]. As the experimental data of the FFM was used intensively in our work, this instrument will be discussed here briefly.

1.2 The Friction Force Microscope

The FFM is based on the AFM and typically consists of a cantilever with an almost atomically sharp tip, see Figure 1.2a. This tip is brought into contact with a clean substrate. Under a constant normal load of typically some nN, the tip is scanned over the surface using an XY-piezo stage. This scanning motion forces the tip to bend laterally, until the force built up in the cantilever is sufficient to make the tip slide over the surface. In most FFM instruments, the deflection of the cantilever is probed using a laser which is pointed at and reflected by the cantilever. The deflection is derived from the shift of the reflected light spot on a split photodiode. By using a four-quadrant photodiode, the normal and lateral forces can be followed simultaneously.
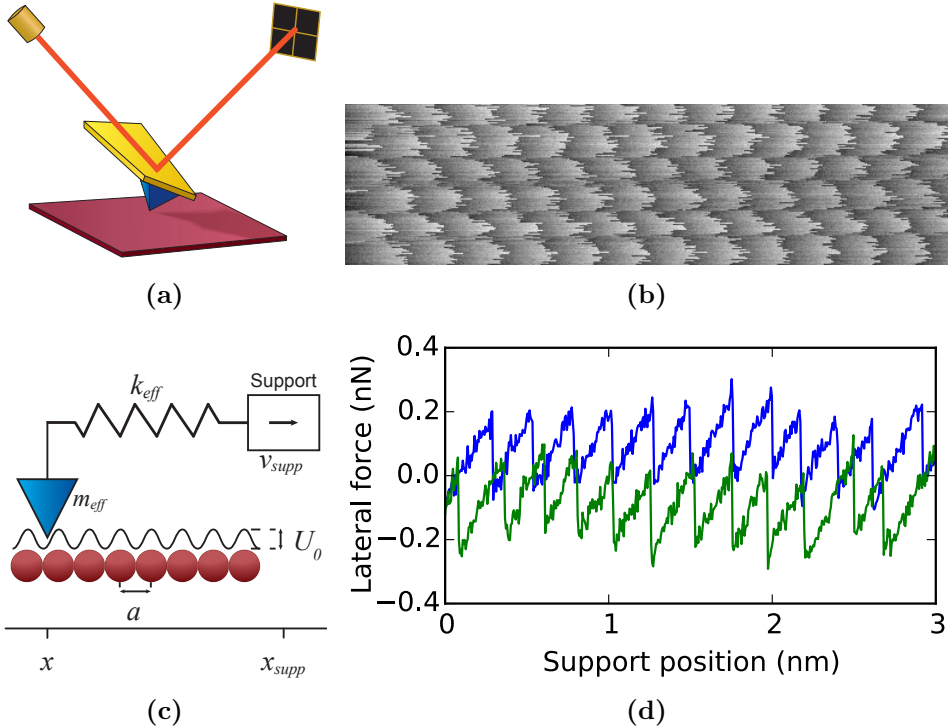
(a)

(b)

(c)

(d)

Figure 1.2: (a) Schematic view of a FFM setup. An atomically scharp tip at the end of a cantilever is pulled over a substrate. The relevant forces are obtained via the cantilever deflection which is measured using a laser and a position-sensitive photodiode. (b) Typical lateral force map ($3 \times 0.8\,\mathrm{nm}^2$), obtained by friction force microscopy[6]. In each line, the silicon-tip moves from left to right over the substrate (in this case HOPG). The gray scale indicates the strength of the opposing lateral force. (c) Schematic view of the FFM experiment; a rigid support (white rectangle) is moving at constant velocity and drags the tip (blue triangle) via a spring over the atomically corrugated substrate (red spheres). The extension of the spring is a direct measure of the lateral force experienced by the tip. (d) Lateral force variation during an individual sweep of the tip from left to right (blue curve; center line in panel (b) and from right to left (green). Panels (b) and (d): data courtesy of Prof. A. Schirmeisen, Justus-Liebig Univerisity, Giessen, Germany

The lateral force data recorded during the scan of the tip over the substrate surface can be plotted as function of the support position, set by the piezo-scanner. Hence, a 2D-image can be constructed easily. This procedure is well established and a typical result of such a measurement is shown in Figure 1.2b. The data in this image was provided by A. Schirmeisen[6].

1.2.1   Stick-slip motion

One feature that is typical for high-quality FFM experiments and that is clearly visible in Figure 1.2b, is a periodic saw-tooth-like variation in the lateral force. In a two-dimensional lateral force map, a lattice emerges that perfectly matches the atomic periodicity of the substrate. A single combination of a forward trace (blue), with the tip running from left to right, and a backward, right-to-left trace (green) of this image is presented in Figure 1.2d. The sawtooth character of these traces is formed by the combination of straight sections in which the lateral force builds up linearly, separated by sections where the lateral force drops abruptly. The sections where the lateral force builds up are associated with configurations in which the tip is effectively stuck in an energy minimum on the corrugated substrate. When the lateral force reaches a threshold value, the tip slips over an energy maximum and ends up in the next energy minimum, one atomic distance further along the substrate. This is why this typical sawtooth-like behaviour is called 'stick-slip motion'.

1.2.2   Modelling a single asperity

Over the years, several theoretical approaches have been constructed to address friction mechanisms. These are ranging from rather simple, mechanical models to more sophisticated concepts, involving phonons[7] or even quantum effects[8]. In spite of all the modelling efforts invested, we are still very remote from having full predictive power with respect to energy dissipation rates and friction coefficients.

The simplest mechanical model, which is extremely popular in the field of nanotribology, is the Prandtl-Tomlinson (PT) model. It is an almost fully deterministic description of a friction contact using a Langevin-type equation of motion[9, 10]. This model appears to be very successful in reproducing experimental data, see e.g. References [6, 11, 12].

1.3   The theoretical model

The core of the PT model is the mass-spring system, as shown in Figure 1.2c. It basically consists of an effective mass, m_{eff}, which is pulled through a corrugated, periodic substrate potential V_{subs} with amplitude U_0. The effective mass is connected to the scanning support via a spring with an effective spring coefficient k_{eff}. In combination, the periodic lattice and the spring result in a total potential with the shape of a corrugated parabola. When the lattice corrugation is sufficiently large, local wells are present in the potential. The model assumes an instantaneous dissipation of the kinetic energy the tip acquires, which results in the tip to be always in one of the (local) minima present. While the support is moving, the spring potential (the parabola) shifts along the corrugated lattice. This results in an emergence and disappearance of the local minima in the corrugated parabola. As soon as the barrier between two local minima has vanished and the tip is in one of these minima, the system is mechanically instable and the tip slips to the next minimum. The observed stick-slip behaviour as shown in Figure 1.2d is characteristic for this fully deterministic model.

The PT model assumes a instantaneous dissipation of energy. In order to make the description of a single asperity contact more mature, a term containing a characteristic energy dissipation rate can be introduced in the model. This would allow us to study the physical dissipation mechanism, which is typically assumed to be linearly dependent on the velocity of the object executing the stick-slip motion. Automatically, the introdution of a dissipative element will add a noise term related to the exchange of energy of the tip with the substrate.

After the introduction of these two dynamic terms, the system can now be described mathematically by the following Langevin equation:

$$m_{\text{eff}}\ddot{x}_{\text{t}} = -\frac{\partial V_{\text{subs}}(x,y)}{\partial x}\bigg|_{(x,y)=(x_{\text{t}},y_{\text{t}})} - k_{\text{eff}}(x_{\text{t}} - x_{\text{support}}) + \xi - \gamma\dot{x}_{\text{t}} \quad (1.2)$$

where x_{t} is the position of the tip. This force-equation expresses the acceleration of the tip as function of four elements: (1) the force of the substrate potential on the tip apex, (2) the effect of the effective spring between tip and support, (3) ξ: the thermal noise on the tip and finally (4) the dissipative element causing the loss of energy that results in the friction force. The reader should note that the values of the dissipation rate γ and the amplitude of the noise term ξ are connected to each other via the fluctuation-dissipation theorem[13]. Further details of the elements 1, 2 and 4 are described in detail in Section 3.3.

As noted earlier, the Langevin model just described can reproduce the observed lateral force traces. This invites us to translate the variables used in the model into physical elements that are present in the experimental setup. During the construction of this translation, it is important to compare both schematics in Figure 1.2.

First we focus on the most important variable: x_t: it is the position of the entity which we denote as the tip. According to Eq. 1.2 the tip makes contact with the substrate and at the other hand, the friction force is calculated by $-k_{eff}(x_t - x_{support})$. Translating to the experiment, the measured friction force, which is deduced from the cantilever spring deflection, is directly related to the position of the tip and hence the tip position can be estimated experimentally.

The effective mass m_{eff} refers not only to the tip atoms that are in direct contact with the substrate, but comprises also the other atoms that are moving together with the tip, which is usually thought to also include a significant fraction of the (much heavier) cantilever.

Another important ingredient is k_{eff}: the effective spring coefficient. A pragmatic, experimental way to determine the effective spring coefficient is by using the stick-slip motion measured by the FFM, as shown in Figure 1.2d. The slope of the lateral force curve during each stick-phase is a direct estimate of the effective spring in the experiment. Typical values found experimentally are around $2\,\text{N/m}$. These values are significantly lower than the lateral/torsional spring coefficients of the cantilevers used (typically $10-200\,\text{N/m}$), indicating that another spring is active in series. There can be several origins of this extra, see Equation 1.3. First, the extra spring can be attributed to the tip, of which the final section is so narrow that it is more flexible than most cantilevers. For an ideally sharp tip, ending in an apex of just a few atoms, we may expect an effective spring coefficient in the order of that of a single interatomic bond, which is indeed in the order of $1\,\text{N/m}$.

A second factor that influences the effective spring coefficient is the tip-substrate interaction (TSI). This interaction results in a force that can be described via a spring coefficient k_{TSI}, which is dependent on many parameters, such as the precise tip apex position and the normal load[14].

A third additional component that affects the effective spring coefficient is the stiffness of the substrate itself, characterized by k_{subs}. As the substrate is a 3-dimensional body consisting of many atoms that are coupled together via atomic bonds, this body is rather stiff. This results in a spring coefficient k_{subs} that will be significantly larger than k_{tip}.

Summarizing, the experimentally observed effective spring coefficient

can be calculated via

$$k_{\text{eff}}^{-1} = k_{\text{cant}}^{-1} + k_{\text{tip}}^{-1} + k_{\text{TSI}}^{-1} + k_{\text{subs}}^{-1} \approx k_{\text{tip}}^{-1} + k_{\text{TSI}}^{-1}. \qquad (1.3)$$

As explained above, k_{cant} and k_{subs} are usually significantly larger than k_{tip}, so their impact on the effective spring coefficient will be minimal. The tip-surface interaction can be manipulated in the experiment via the normal load. Relatively high normal loads make k_{TSI} high, which makes k_{eff} approximately equal to k_{tip}. This provides an excellent recipe to estimate the k_{tip} experimentally[14], which is the case we will deal with in the next chapters. Hence, in our work, we can assume that $k_{\text{eff}} \approx k_{\text{tip}}$.

1.3.1 Towards a 2-mass-2-spring model

The need to resort to an effective spring coefficient, described above, indicates that the simple description of the dynamics of a single mass, given by Equation 1.2, falls short of capturing the full dynamics that is at play. Instead of a single mass (tip + part of the cantilever) dragged through the potential energy landscape via a single spring (Figure 1.2c), we are dealing with two springs in series (cf. Equation 1.3) and, hence, also with two masses. One of them, to be associated with the tip, is necessarily small, while the other, associated with (a large part of) the cantilever, must be much larger. We should expect that the massive cantilever will not be able to follow the probably much more rapid dynamics of the tip. Since the force signal in FFM-measurements is obtained from the cantilever deformation, we should expect that much of the actual contact dynamics is not appropriately reflected in the recorded forces.

The need of a more refined description of a friction contact was realized a few years ago, leading to a small number of models with two or more springs. S. Maier et al. reported a nice combination of results from high frequency data sampling experiments with simulations using a two-mass-two-spring model[15]. Their results hint that highly time resolved research is crucial for further understanding the friction contact behaviour. Also the work of Abel et al. indicates that friction is a very dynamic phenomenon asking for attention to extremely rapid evolving processes[16].

In the following chapter, we will critically evaluate the common interpretation and simulations in order to identify a discrepancy which is inherent in most models reported so far. We will be forced to change our understanding of the contact dynamics and the mechanism of energy dissipation.
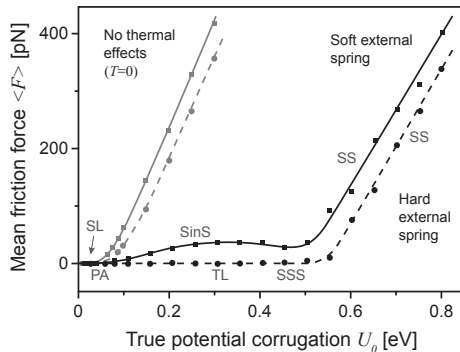
Figure 1.3: The calculated mean friction force as function of the corrugation potential, picture reprinted from [17]. Several friction regimes emerge, depending on the calculation parameters. The open symbols denote calculations without thermal effects $(T = 0)$, the external spring is the cantilever spring. The stick-slip (SS), superlubric (SL) and thermolubric (TL) regimes are discussed in the text briefly. The other regimes present are stochastic stick-slip (SSS), stuck in slipperiness (SinS), slipping via an intermediate position (SIP) and 'passive apex' (PA). A detailed description of all the friction regimes is given in the original publication.

1.4   A first look at 2-mass-2-spring behaviour

Incorporating a second spring and a second mass into the description of a single-asperity friction contact, introduces a wealth of dynamic phenomena in the combined motion of the cantilever and the tip. This rich dynamics has been explored theoretically intensively, of which a comprehensive overview is present in Reference [17]. Depending on e.g. the lattice constant, the temperature, the masses of tip and cantilever and the two spring coefficients different friction behaviour is observed. A graphical overview of these friction regimes is presented in Figure 1.3, which is reproduced from Reference [17]. This figure shows a surprisingly large number of friction regimes, each indicated by one of the acronyms. Here we briefly mention the three most relevant ones.

Stick-slip (SS)   Stick-slip motion is the motion introduced before, in which the tip is periodically trapped in a potential well and is forced to slip through the potential energy landscape, lattice spacing by lattice spacing. This type of motion occurs when the amplitude of the tip-substrate potential is sufficiently high with respect to the effective spring coefficient, when the temperature is sufficiently low, and when the dissipation rate at the

tip-substrate contact is sufficiently high. It is observed in a large fraction of FFM experiments.

Superlubricity (SL)   When the amplitude of the tip substrate potential is lowered enough with respect to the effective spring coefficient, sliding proceeds without slip-instabilities and the friction force is reduced nearly to zero. This situation can be realized either by reducing the normal force between tip and substrate, typically requiring one to exert a negative normal force (to compensate part of the tip-substrate attraction)[14], or by shaping the contact in the form of an incommensurate interface between two crystalline lattices[1, 18]. The latter geometry is known under the name 'superlubricity'[19].

Thermolubricity (TL)   Another regime of extremely low friction arises when the corrugation of the tip-substrate interaction potential is sufficiently low with respect to the thermal energy that the tip overcomes the energy barriers between neighbouring energy minima frequently on the timescale of the support motion. This leads to a kind of biased diffusion of the tip with hardly any energy dissipation. This regime of thermally assisted motion has been introduced under the name 'thermolubricity'[20].

Throughout the first part of this thesis, when needed, specific aspects of the friction regimes will be discussed and characterized in more detail.

1.4.1   Focus of this part of the thesis

The theoretical approaches listed here do reproduce experimental data quite often. However, they still contain subtle assumptions or hidden contradictions. This thesis will first elaborate on the conventional interpretation of FFM-data using the Prandtl-Tomlinson model. We will show that this interpretation hides a fundamental contradiction. Via an estimate of the order of magnitude of the dissipative forces required to produce atomic-scale patterns in the so-called stick-slip motion of a friction nano-contact, we find that the energy dissipation must be dominated by a very small, highly dynamic mass at the very end of the asperity. Based on these findings, a more physical, but still rather simple method to describe the single-asperity contact will be presented. The evaluation of this method casts new light on the behaviour of sliding surfaces and invites us to speculate about new ways to control friction by manipulation of the contact geometry.